Journal of Applied Electrochemistry **32**: 811–818, 2002.

Properties of silver–antimony alloys electrodeposited from ferrocyanide–thiocyanate electrolytes

I. KRASTEV[1,*], N. PETKOVA[1] and A. ZIELONKA[2]
[1]*Institute of Physical Chemistry, Bulgarian Academy of Sciences, 1113 Sofia, Bulgaria*
[2]*Forschungsinstitut für Edelmetalle und Metallchemie, 73525 Schwäbisch Gmünd, Germany*
*(*author for correspondence)*

Received 23 October 2001; accepted in revised form 16 April 2002

Key words: coating properties, electrodeposition, ferrocyanide–thiocyanate electrolyte, internal stress, silver–antimony alloy

Abstract

The influence of electrolysis conditions on the internal stress, microhardness, electrical contact resistance, wear resistance, roughness, and friction properties of silver–antimony alloys deposited from ferrocyanide–thiocyanate electrolytes is studied. The internal stress of the coatings depends strongly on their antimony content. Stress changes and transition from compressive to tensile stress at increased antimony content in the alloy are observed. By internal stress measurements, conclusions can be drawn concerning the homogeneity or heterogeneity of the coating, that is, whether the coating consists of one or two phases. The changes in microhardness are related to variations of the internal stress and to the phase transition. The codeposition of antimony leads to a reduction of the coating roughness. Increased Sb content of the alloy leads to an increase in the electrical contact resistance and to reduction of the contact forces and wear resistance of the coatings. At large deviations from equilibrium, an oscillating electrochemical reaction is observed leading to space-time structures on the electrode surface.

1. Introduction

Interest in the electrodeposition of silver–antimony alloys is based on the possibility of depositing layers of improved mechanical and tribological properties compared to the pure silver coatings [1–4], and also studying the self-organization phenomena under electrochemically well controlled conditions [5].

Electrodeposition of silver–antimony alloys is usually carried out from cyanide electrolytes [1–4]. As an alternative, lower toxicity, ferrocyanide–thiocyanate electrolytes have been used, whereby the process is realized in the absence of free cyanide [6]. The electrolytes were prepared by a complicated procedure [3] and the precise concentration of the ferrocyanide ions was not always known. Considerable amounts of thiocyanate ions were added to this electrolyte to serve as depassivator for the anode [7]. The electrochemical properties of this type of electrolyte have been described in detail [6–14].

The elemental and phase composition of the alloy layers has been investigated [15]. The codeposition of small amounts of antimony results in the formation of a silver-rich solid solution (α-phase) with an increased lattice parameter [15]. After saturation of the silver lattice by antimony, deposition starts of a second phase richer in antimony. Under certain conditions, formation and propagation of ordered structures of the two phases were observed on the surface [5, 16–19]. The causes of the formation of the space-time structures were discussed previously [5, 14, 18, 19].

However, some properties of these alloy layers, which are of practical interest, such as internal stress, hardness, roughness, wear resistance, electrical resistance, and friction properties are not well known. The aim of the present paper is to obtain data on the mechanical, electrical and tribological properties of the silver–antimony alloy deposited from ferrocyanide–thiocyanate electrolytes.

2. Experimental details

The method of preparation of the electrolyte is described elsewhere [3, 6, 7] and some of its electrochemical properties were discussed recently [11]. The electrolyte composition is given in Table 1.

The electrochemical measurements were carried out in a 50 cm^3 glass cell with a platinum cathode (0.4 cm^{-2}) and two silver anodes. The reference electrode (Ag/AgCl) was connected to a Haber–Luggin capillary by a bridge filled with a solution of 3 M KCl. Measurements were performed by a computer-controlled PAR potentiostat/galvanostat model 263A, using the SoftCorr II software.

The internal stress, *IS*, was monitored with the apparatus constructed by Stalzer [20], operating on the

Table 1. Electrolyte composition

Component	Concentration/g dm^{-3}
Ag	16
$K_4Fe(CN)_6 \cdot 3H_2O$	70–90
K_2CO_3	20
KSCN	150
$KNaC_4H_4O_6 \cdot 4H_2O$	60
Sb as $K(SbO)C_4H_4O_6 \cdot \frac{1}{2}H_2O$	2.5–10

principle of the one-sided galvanized bendable cathode. During electrodeposition, the cathode is bending in a specific direction depending on whether the induced internal stress is compressive or tensile. A sensor detects the deviation and compensates it through an electric feed back system. The force needed for compensation and hence the value of the internal stress is deduced from the electrical signal. The latter is transferred through a suitable interface to a computer for monitoring and processing and is depicted as the ordinate in Figures 2, 3, 5–7.

The method permits *in situ* monitoring of the internal stress during electrodeposition. The value of the internal stress is given by

$$S = \frac{4FL}{3btd}$$

with: S/N mm^{-2} the stress in the coating; F/mN the force exerted on the sensor determined from the change in the electrical signal during deposition ($\Delta U = U - U_0$) by taking into account an apparatus calibration constant; L/mm the distance between the contact point of the sensor on the sample and the level of the sample holder; b/mm the sample width, t/mm the thickness of the sample plate; and d/μm the thickness of the coating.

By combining the parameters of the electrodes used and the apparatus constant into a constant K, the above expression is reduced to

$$S = K\frac{\Delta U}{d}$$

which gives the relation between the sensor signal, the coating thickness and the internal stress.

The cathodes were 9 cm long, 1 cm wide, 0.3 mm thick and their backsides were lacquer-insulated. Silver was deposited along 7 cm of the plate, dipped in the electrolyte (400 cm^3). The thickness of the deposited coating and the rate of deposition were determined by the mass increase. The density of the coating was assumed to be equal to that of pure silver. Rough estimations proved that the largest possible error in the determination of *IS* was about 7% for 20 wt% Sb in the coating. Before deposition the samples were electrochemically degreased in an alkaline medium, then neutralized and precoated with several micrometres of silver to avoid contact deposition on the copper substrate.

The microhardness, H_v, of the deposited coatings was measured with the Leitz apparatus Durimet II using a load of 245, 2 mN at three positions set at a distance of 2 cm from each other. Each point of the curves in Figure 9 represents the average of at least nine measurements.

The average value of the roughness, R_a, of the deposited layers was determined by a Perthen profilometer Perthometer.

The contact resistance, R_Ω, of 6 μm thick layers was measured by the Burster microohmmeter Resistomat 2323 on brass contact pins of diameter 4 mm and length 14 mm at a pressure force of 2 N. After the standard pretreatment (electrochemical degreasing, rinsing and neutralization), the pins were coated with Ag–Sb alloy in an electrolyte with silver concentration $C_{Ag} = 16$ g dm^{-3} and antimony concentration $C_{Sb} = 7.5$ g dm^{-3}. As reference samples, other pins were initially coated with nickel (60 °C, 5 A dm^{-2}, 5 min) and then with gold in the electrolyte Auruna 539 of Degussa (50 °C, 2.5 A dm^{-2}, 5 min).

The contact forces, F, were measured during the introduction of similar contact pins coated with a 6 μm thick deposit of Ag–Sb alloy into pure silver coated jacks. For this purpose, an apparatus constructed by FEM was used. A sensor determined the compressive and tensile forces and another sensor for the distance. Using the Labtech program, the response was transferred through suitable interface modulus to a computer. During the measurements, the pin was introduced into the jack at a constant velocity and the changes of the applied force with time were recorded. The system was calibrated so that a force of 32 N corresponded to a signal of 1 mV. The contact forces were assumed to be negative when the pin was introduced into the jack.

After measurement of the internal stress, the wear resistance, A, of the same layers was determined by the Bosch–Weinmann method. An abrasive disc (dia. 47 mm, width 10 mm) moves under constant load (3.92 N) back and forth on the tested surface. After each cycle, the disc rotates in a small step, so as to provide fresh abrasive surface. By appropriate choice of the grain size of the abrasive band, it is possible to control the intensity of abrasion. In the present study, the latter was determined after 400 cycles using an abrasive band of grade 1000. The wear resistance was determined by the weight loss. It is defined as the number of cycles required for the removal of 1 mm^3 of the coating and is given by

$$A = z(D/G)$$

with A the wear resistance; D/mg mm^{-3} the density of the material; z the number of cycles, and G/mg the weight loss.

3. Results and discussion

3.1. *Electrochemical investigations*

The process of electrochemical deposition and dissolution of silver in the electrolyte utilized was described in

detail [11]. Figure 1 (dashed line) shows the cyclic voltammetric curve obtained in the absence of antimony. The two cathodic reactions before the occurrence of hydrogen evolution and the two anodic reactions are well expressed. The high concentration of thiocyanate ions causes the complete dissolution of the silver deposited during the cathodic period.

Addition of antimony to the electrolyte leads to changes in the curve (Figure 1, solid line). The cathodic maximum of the first reaction of silver deposition is still observed as a hump in this case. However, instead of the second cathodic maximum of silver, a new one appears, corresponding to the simultaneous deposition of both metals. This new phase grows with a higher rate than that of pure silver and the respective current densities are also higher.

During dissolution, the position and height of the first anodic maximum remain unchanged when scanning up to different cathodic potentials. This confirms our previous assumption that, at this anodic potential, a layer of insoluble AgCN covers the electrode surface. The next maxima correspond to silver dissolution (IIa), dissolution of Ag–Sb alloy (IIIa) and oxidation of Fe^{2+} to Fe^{3+} (IVa) on the platinum surface [11].

3.2. *Internal stress*

The changes in *IS* during electrodeposition are illustrated in Figure 2 for different current densities, *J*, in an Sb-free electrolyte. For thick silver layers, *IS* is positive (tensile stress) and increases with *J*. At $C_{Ag} = 16$ g dm^{-3} and $J = 0.75$ A dm^{-2}, rough layers are obtained and *IS* cannot be measured precisely since the deposit thickness cannot be defined with sufficient accuracy.

The codeposition of small amounts of antimony leads to the formation of a solid solution (α-phase) and to a increase in the silver lattice parameter [15]. Compressive stress is observed in this case. Changes in both the value

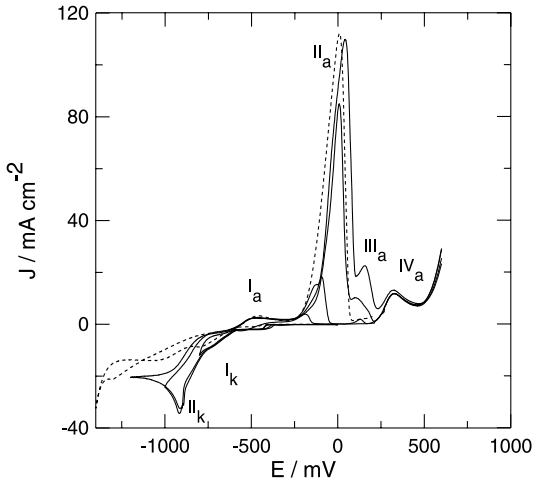

Fig. 1. Cyclic voltammetric curves in Ag and Ag–Sb electrolytes. $v = 25$ mV s^{-1}; $C_{Ag} = 16$ g dm^{-3}; (- - - -) $C_{Sb} = 0$ g dm^{-3}; (—) $C_{Sb} = 5$ g dm^{-3}.

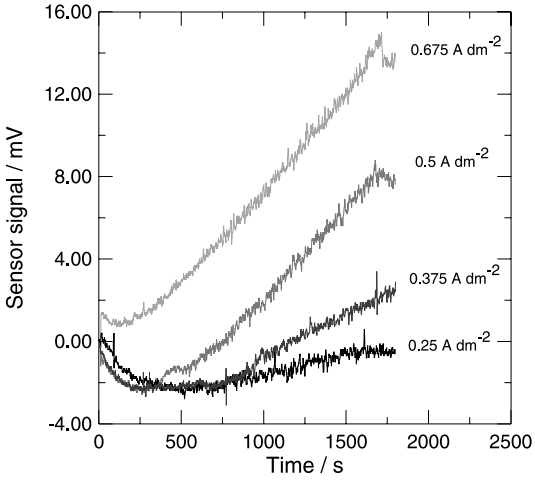

Fig. 2. Changes of the sensor signal with time at various *J* values during Ag deposition. $C_{Ag} = 16$ g dm^{-3}; $C_{Sb} = 0$ g dm^{-3}.

and the sign of *IS* (tensile stress) are observed at higher Sb contents in the deposit.

Figure 3 shows the variations of *IS* for different antimony concentrations. Due to the codeposition of

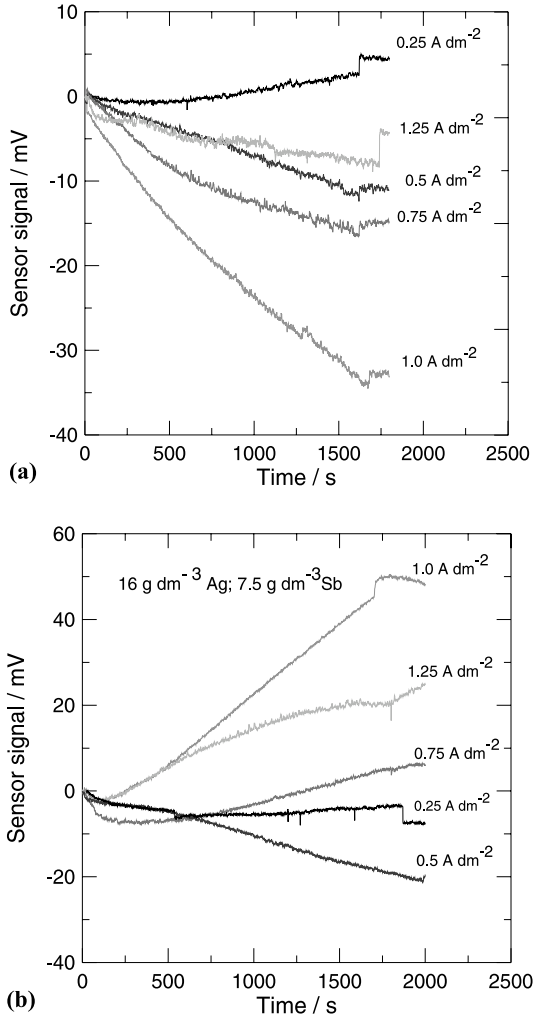

Fig. 3. Changes of the sensor signal with time during alloy deposition at various *J* and C_{Sb} values. (a) $C_{Sb} = 2.5$ g dm^{-3}; (b) $C_{Sb} = 7.5$ g dm^{-3}.

Sb, the internal stress has turned negative (compressive) (Figure 3(a)). It increases rapidly with J (i.e., with the Sb content in the deposit), reaching a maximum at $J = 1$ A dm^{-2} for C_{Sb} of 2.5–5.0 g dm^{-3}. A further rise in J (1.25 A dm^{-2}) leads to a rapid decrease of the compressive stress, which, on the basis of previous studies, could be attributed to saturation of the silver lattice with antimony and deposition of a new phase with higher Sb content simultaneously with the α-phase [15]. The changes in the curves just before the end of the experiment are due to the current interruption. At higher C_{Sb}, a higher current density can be achieved, thus enabling the codeposition of larger Sb quantities in the coating. However, in this case, the saturation of the silver lattice with Sb is achieved at a lower current density. Thus for $C_{Sb} = 7.5$ g dm^{-3}, (Figure 3(b)), compared to the lower antimony concentration (Figure 3(a)), not only a reduction of *IS* can be established but it becomes tensile as in the case of pure silver layers. This variation of *IS* could be related to further changes in the phase composition at higher Sb content in the coatings. The formation of a new phase with the increase of J up to 1 A dm^{-2} ($C_{Sb} = 7.5$ g dm^{-3}) was actually detected by X-ray diffraction (Figure 4). The further increase of J up to 1.25 A dm^{-2} leads to deposition of larger quantities of this phase, which allows its better identification (Figure 4), and to further changes in the internal stress (Figure 3(b)). In addition, the increase of J contributes to the improved perfection of the ⟨111⟩ texture of the α-phase (Figure 4).

At a still higher antimony concentration ($C_{Sb} = 10$ g dm^{-3}), compressive stress is observed at low current density ($J < 0.5$ A dm^{-2}) and tensile stress is observed at high current density ($J = 0.75$–1.5 A dm^{-2}).

Figure 5 shows the variation of *IS* at $J = 0.75$ A dm^{-2} for different antimony concentrations. At low C_{Sb} (2.5 to 5 g dm^{-3}), the codeposited Sb participates with Ag in the formation of the solid solution (α-phase). At higher C_{Sb} (7.5–10 g dm^{-3}) the excess quantity of the deposited Sb is included in the second phase; the stress changes its sign and becomes tensile. This means that by measuring the *IS* at a specific J value (e.g., 0.75 or 1 A dm^{-2}) the transition from single-phase to double-phase electrodeposits can be detected. Hence, on the basis of the *IS* diagram it could be established whether a coating is homogeneous or heterogeneous. The homogeneous Ag–Sb coatings exhibit a compressive *IS*, while the heterogeneous layers exhibit a tensile one.

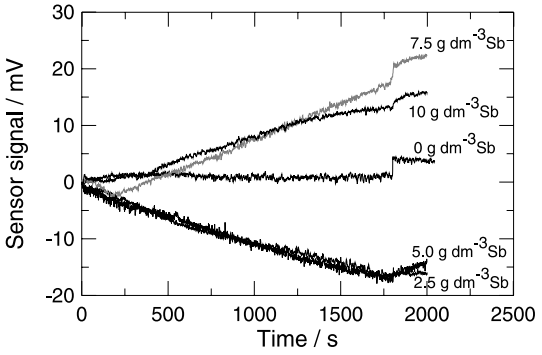

Fig. 5. Sensor signal during alloy deposition as dependent of C_{Sb} at constant current density. $J = 0.75$ A dm^{-2}.

In some cases, significant *IS* changes can be observed during deposition. Figure 6 shows that the presentation of the results as the output voltage of the sensor is more informative than the calculated values of *IS*. A transition is observed from compressive to tensile *IS* due to changes in the deposition conditions. The initial compressive *IS* corresponds to a bright coating, while the subsequent tensile *IS* corresponds to a dull coating due to depletion of Sb in the electrolyte and deposition of Ag-richer layers. However, this curve shows the possibility of successful application of the method for investigation of the *IS* during deposition of multilayer systems consisting of layers with different elemental or phase compositions.

Figure 7 shows again that the *IS* measurement leads to indirect conclusions concerning the depletion of the alloying component Sb in the electrolyte. Curve (a) corresponds to a freshly prepared electrolyte ($C_{Sb} = 7.5$ g dm^{-3}), while curve (b) illustrates the situation at a

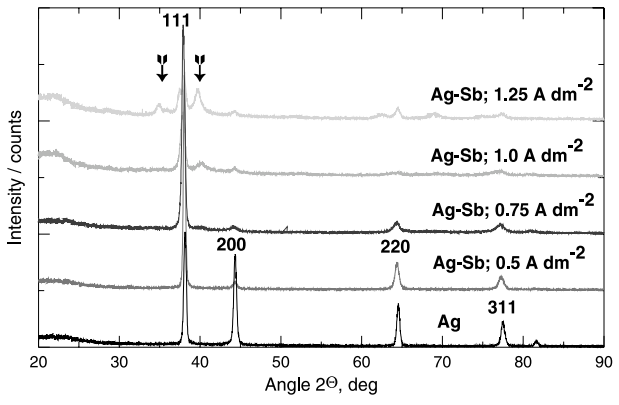

Fig. 4. X-ray diffractograms of Ag and Ag–Sb alloy coatings at various J values. $C_{Ag} = 16$ g dm^{-3}; $C_{Sb} = 7.5$ g dm^{-3}.

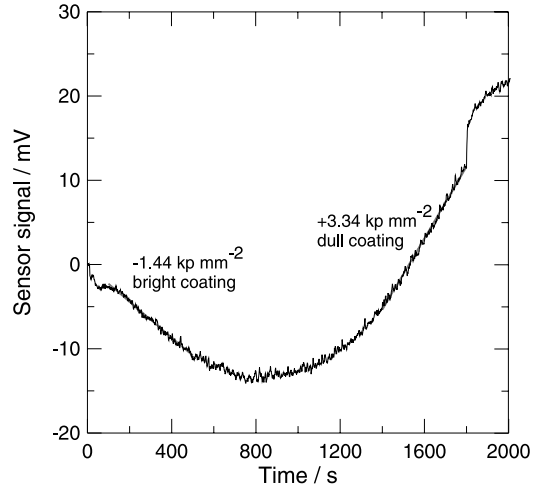

Fig. 6. Transition from compressive to tensile stress in the coating in an exhausted electrolyte: C_{Sb}(initial) = 7.5 g dm^{-3}; $J = 1$ A dm^{-2}.

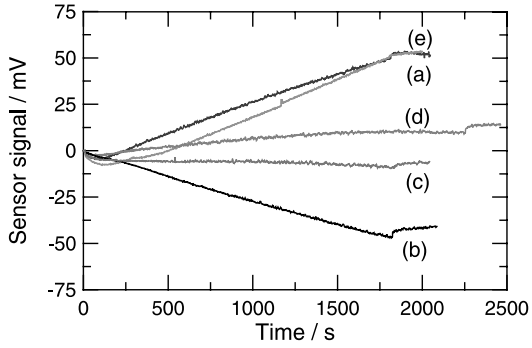

Fig. 7. Effect of the variations in C_{Sb} on the internal stress; $C_{Ag} = 16$ g dm^{-3}; $J = 1.0$ A dm^{-2} (a) freshly prepared electrolyte; $C_{Sb} = 7.5$ g dm^{-3}; (b) exhausted electrolyte; (c) exhausted electrolyte + 2.5 g dm^{-3} Sb; (d) exhausted electrolyte + 4.8 g dm^{-3} Sb; (e) exhausted electrolyte + 7.3 g dm^{-3} Sb.

much lower C_{Sb} at $J = 1$ A dm^{-2}. The *IS* variations are clearly seen: after Sb depletion *IS* is transformed from tensile to compressive. By the addition of the respective quantities of antimony in the electrolyte, the reverse transition from homogeneous to heterogeneous coatings can be realized and the compressive stress can be changed again to tensile, its value becoming approximately the same as that observed in the freshly prepared electrolyte.

3.3. *Rate of deposition*

Figure 8 shows the rate of deposition, V, of Ag–Sb alloy against the current density calculated from the weight of the deposited layer, assuming that the latter consists of pure silver. Average values of the results obtained for all investigated C_{Sb} are used. At higher J, a deviation from linearity is observed, which can be assigned, on the one hand, to the increased Sb content in the deposit under such conditions and, on the other hand, to the less accurate determination of the thickness due to deposition of rougher coatings.

3.4. *Microhardness*

Microhardness, H_v, is a structure sensitive property of every alloy and depends on the composition of the alloy

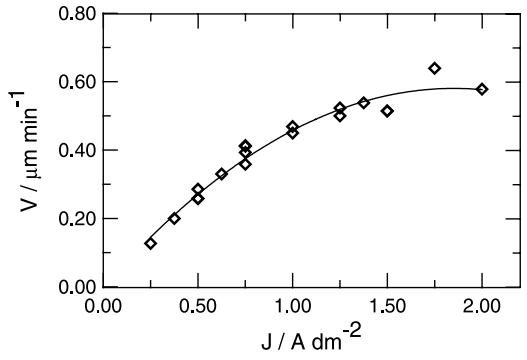

Fig. 8. Rate of deposition, V, of the alloy layers against current density.

layers. Figure 9 shows the variations of H_v of the coatings against J at various C_{Sb}. For obvious reasons, large deviations in the deposition near the limiting current density are observed both for pure silver and for alloy layers. However, it is established that the codeposition of antimony leads to an increase in H_v. For $C_{Sb} = 2.5$–5 g dm^{-3}, the maximum value of H_v is observed at $J = 1$ A dm^{-2}, which corresponds to the maximum value of the compressive *IS* in these coatings (Figure 3(a)). At higher C_{Sb} the maximum *IS* values are detected at higher current density ($J = 1.5$–1.75 A dm^{-2}), which in this case corresponds to the maximal tensile stress in the coatings. The H_v curve for $C_{Sb} = 7.5$ g dm^{-3} has a peculiar behaviour, which requires additional detailed investigations.

3.5. *Roughness*

The codeposition of Sb exerts a brightening effect on the deposited coatings. Increase in its content in the alloy leads to the disappearance of the milky-white silvery appearance of the coatings and they become semi bright. Only at higher J, when the Sb-richer phase is codeposited, do they turn grey and shiny. In these bright coatings, ordered structures of phases with different Sb contents are observed (Figure 14).

The results of the roughness measurements are displayed in Figure 10. R_a represents the average value of the roughness profile along the measured line. In the Sb-free silver coatings, R_a increases with J. During the codeposition of antimony, due to its effect of brightening and grain size reduction, the R_a increase is suppressed and smooth coatings are obtained over the entire range of J values. Naturally, at high J values close to the limiting current density, the alloy layers turn rough and black.

The results show that no influence could be expected of the alloy coating roughness on their other properties, such as electrical contact resistance, contact forces, or wear resistance.

3.6. *Contact resistance*

The contact resistance, R_Ω, of the Ag–Sb coatings increases at increased J, that is, at a higher Sb content in the deposit [3]. A linear dependence R_Ω/J was established by measurements of the alloy coatings against a gold-plated substrate. The slope of this curve was less steep than that of the curve obtained by measurements against alloy samples of the same composition (Figure 11). In the latter case, deviations from linearity are observed at low J values where pure Ag is deposited with only traces of Sb. Under such conditions (i.e., at lower Sb content in the deposit), the contact resistance measured against the same alloy is lower than that against the gold-plated sample. At higher current density ($J > 0.9$ A dm^{-2}), the worsening effect of the codeposited Sb in both alloy samples is combined and this results in higher values of R_Ω compared to the

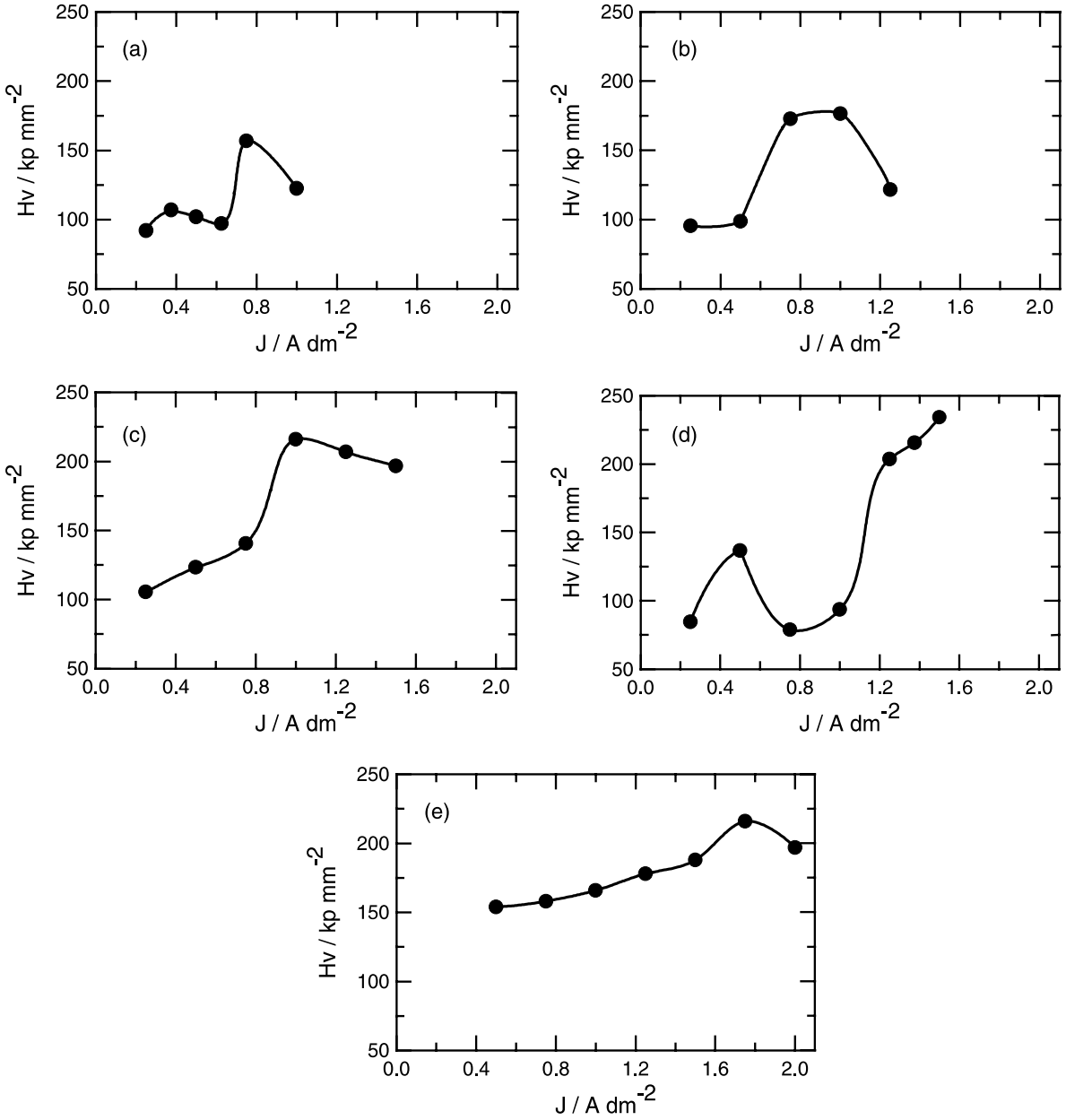

Fig. 9. Microhardness, H_v, of the alloy layers against J at various Sb concentrations. $C_{Ag} = 16$ g dm^{-3}. C_{Sb}: (a) 0, (b) 2.5, (c) 5.0, (d) 7.5 and (e) 10.0 g dm^{-3}.

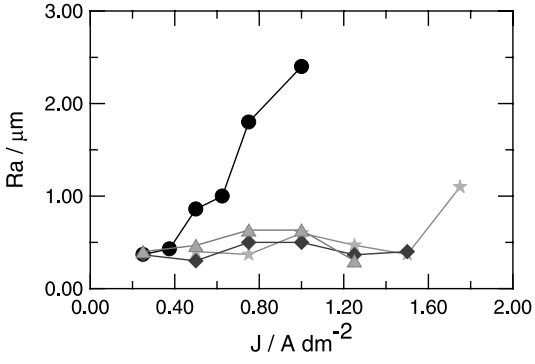

Fig. 10. Average roughness, R_a, of Ag and Ag–Sb coatings against J at various Sb concentrations. $C_{Ag} = 16$ g dm^{-3}. C_{Sb}: (●) 0, (▲) 2.5, (♦) 7.5 and (★) 10.0 g dm^{-3}.

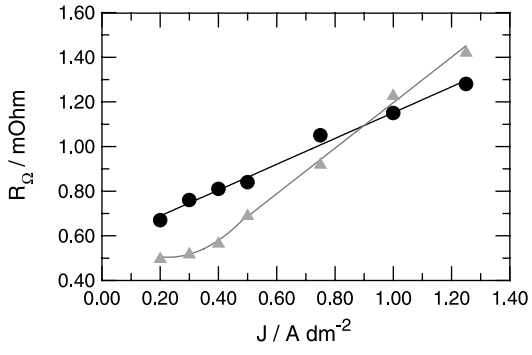

Fig. 11. Contact resistance, R_Ω, of 6 μm alloy layers. $C_{Ag} = 16$ g dm^{-3}; $C_{Sb} = 7.5$ g dm^{-3}. Key: (●) against gold and (▲) against the same alloy.

measurements against gold-plated substrate. In this case, the coating consists not only of the solid solution (α-phase) but it is heterogeneous and a part of the surface is occupied by the Sb-richer phase, which is in good agreement with the other properties of the coatings (compare Figures 3(b), 4, 9, 12, 13). Obviously, the electrical conductivity of this phase is considerably worse than that of silver, or gold.

3.7. *Contact forces*

The force, F, measured upon introduction of the pin into the jack increases proportionally to the contact area and reaches a maximum when the pin is fully inserted into the jack. This maximum value is shown in Figure 12 as a function of current density at which the coating is deposited. F decreases with the rise in current density due to increased Sb content in the alloy. A stronger reduction is detected in the case of heterogeneous two-phase layers deposited at high current densities, compared to the homogeneous α-phase alloys, which is probably due to the lubricating properties of the Sb-richer phase.

Taking into account the dependence of F on the contact area, that is, bearing in mind that the maximum value of the contact force would be different for pins and jacks with the same properties of the coating, but of different size, the slope of the time dependence of F could also be proposed as a measure of the friction properties (contact forces) of the coatings obtained.

3.8. *Wear resistance*

In the absence of antimony, the coatings exhibit high wear resistance, A (Figure 13), which becomes still higher when small quantities of antimony are codeposited in the coating at low C_{Sb} (2.5 g dm^{-3}) and at low current density (0.5–0.75 A dm^{-2}). At high J and the same C_{Sb}, the coatings grow rough and the results are unreliable.

At high C_{Sb}, a surprising reduction in the wear resistance is obtained with increase in J, that is, in the Sb content in the coating. The values are several times lower for the heterogeneous layers deposited at high J. This is due to the mechanical properties of the Sb-richer phase. Additionally, the coatings deposited under such conditions display positive *IS* where blistering of the coating could occur more readily than in the case of compressive stress.

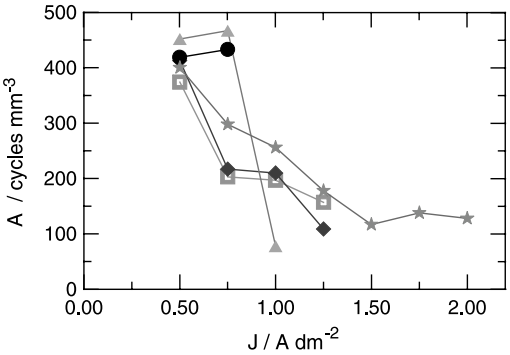

Fig. 13. Wear resistance, A, against current density at various Sb concentrations. $C_{Ag} = 16$ g dm^{-3}. C_{Sb}: (●) 0; (▲) 2.5; (♦) 5.0; (□) 7.5 and (★) 10.0 g dm^{-3}.

It can be concluded that the heterogeneity of the layers of high Sb content leads to worsening, not only of electrical properties, but also of wear resistance.

By codeposition of Sb, semibright to bright coatings of low roughness can be obtained. Under certain conditions, the different phases on the coating surface can self-organize in ordered structures, as shown in Figure 14. In this case, the electrochemical system passes into an oscillating state; during deposition under potentiostatic conditions, oscillations of the cathodic current are observed (Figure 15). The oscillation period is related to the period of the developed wave structures and decreases at higher potentials. This observation shows that layers with high antimony content, which are not current practice today, could be of considerable scientific importance.

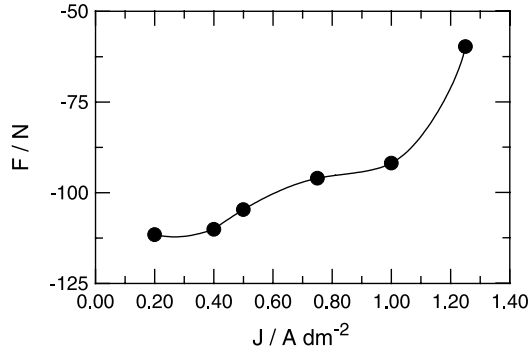

Fig. 12. Contact forces, F, of 6 μm alloy layers against current density. Measurements against silver-plated jacks. $C_{Ag} = 16$ g dm^{-3}; $C_{Sb} = 7.5$ g dm^{-3}.

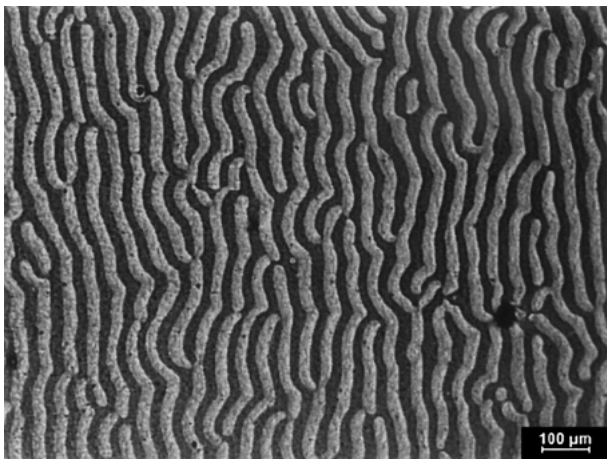

Fig. 14. Ordered structures of phases of various Sb contents resulting from self-organization phenomena during the oscillating electrode reaction. $C_{Ag} = 16$ g dm^{-3}; $C_{Sb} = 7.5$ g dm^{-3}; $KAg(CN)_2$ electrolyte; 1.25 A dm^{-3}; 12 μm.

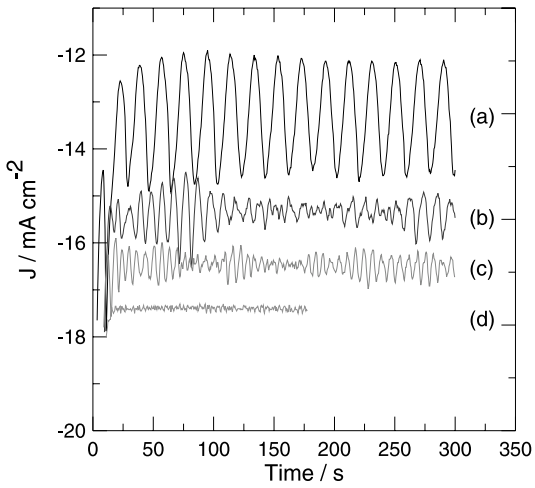

Fig. 15. Current oscillations with time at different cathodic potentials. $C_{Ag} = 18$ g dm^{-3}; $C_{Sb} = 5$ g dm^{-3}. Reference electrode Ag/AgCl. Cathodic potential: (a) −885, (b) −900, (c) −910 and (d) −920 mV.

4. Conclusions

The addition of Sb to the silver-plating electrolyte leads to electrochemical instability and simultaneous deposition of phases with different Sb contents, which under certain conditions can organize themselves in ordered structures.

In the absence of Sb, the silver layers exhibit positive (tensile) internal stress, which increases with the increase in the cathodic current density.

By Sb codeposition, the silver lattice becomes strained. Negative (compressive) internal stress develops in the coatings and increases with the rise in the current density. After saturation of the silver lattice with Sb, deposition of another Sb-richer phase takes place, which can be detected by X-ray measurements, and the internal stress decreases. At higher Sb-content in the coating, tensile stress is again observed.

The method used for the *in situ* measurement of the internal stress provides information about the antimony concentration in the electrolyte and the phase homogeneity of the deposited layers.

The microhardness of the deposited alloy layers depends on the codeposition of Sb and increases at higher Sb content in the deposit. Significant H_v changes are detected in the range of J values where the changes in the internal stress are greater due to the deposition of the Sb-richer phase.

By the codeposition of antimony, coatings are obtained which are smoother and brighter than those of pure silver.

The electrical contact resistance increases at higher Sb content in the coating, its changes being more significant when measured against the same alloy than against gold-plated samples.

The contact forces measured on pins and jacks decrease at higher current density, that is, at higher Sb content in the coating. They become rather small in heterogeneous alloys consisting of two phases, since the Sb-richer phase improves the sliding properties of silver, but the wear resistance of the alloy layers decreases.

Acknowledgements

The present studies are part of a joint research project between the Institute of Physical Chemistry, Bulgarian Academy of Sciences, Sofia, and Forschungsinstitut für Edelmetalle und Metallchemie, Schwäbisch Gmünd. The authors express their gratitude to Deutsche Forschungsgemeinschaft for the financial support of project 436 Bul 113/97/0-2.

References

1. M. Luce and D.G. Foulke, *in* F.A. Lowenheim (Ed.) 'Modern Electroplating' (J. Willey & Sons, New York, 3rd edn, Interscience, 1974), chapter 14, p. 358.
2. A. Brenner, 'Electrodeposition of alloys', Vol. 1 (Academic Press, New York, 1963), p. 609.
3. P.M. Vjacheslavov, S.J. Grilihes, G.K. Burkat and E.G. Kruglova, '*Galvanotechnika blagorodnih i redkih metallov'* (Mashinostroenie, Leningrad, 1970), p. 5 (in Russian).
4. P.M. Vjacheslavov, '*Novie elektrokhimicheskie pokritija*', (Lenizdat, Leningrad, 1972), p. 213 (in Russian).
5. I. Krastev and M. Nikolova, *J. Appl. Electrochem.* **16** (1986) 875.
6. N.P. Fedotjev and V.A. Ilin, *Zh. Prikl. Khim.* **36**(8) (1963) 1763 (in Russian).
7. V.G. Kakovkina, V.K. Gabidulina and E.I. Iljushina, *Elektrokhimija* **7**(8) (1971) 1140 (in Russian).
8. V.A. Kajkaris, I. Ju. Pivorjunajte and V.V. Markushas, *Elektrokhimija* **2**(2) (1966) 234 (in Russian).
9. T.Ju. Jankauskas, V.Ju. Skuchas and V.A. Kajkaris, *Zh. Prikl. Khim.* **45**(12) (1972) 2747 (in Russian).
10. Z. Napuch and E.A. Nechaev, *Elektrokhimija* **9** (1973) 1020 (in Russian).
11. I. Krastev, A. Zielonka, S. Nakabayashi and K. Inokuma, *J. Appl. Electrochem* **31**(9) (2001) 1041.
12. I. Krastev, M.E. Baumgärtner and Ch.J. Raub, *Metalloberfläche* **46**(2) (1992) 63.
13. I. Krastev, M.E. Baumgärtner and Ch.J. Raub, *Metalloberfläche* **46**(3) (1992) 115.
14. S. Nakabayashi, I. Krastev, R. Aogaki and K. Inokuma, *Chem. Phys. Lett.* **294** (1998) 204.
15. I. Kristev and M. Nikolova, *J. Appl. Electrochem.* **16** (1986) 867.
16. I. Krastev, M. Nikolova and I. Nakada, *Electrochim. Acta* **34** (1989) 1219.
17. I. Krastev, *Bulg. Chem. Commun.* **29**(3/4) (1996/97) 586.
18. I. Krastev and M.T.M. Koper, *Physica A* **213** (1995) 199.
19. S. Nakabayashi, K. Inokuma, A. Nakao and I. Krastev, *Chem. Lett.*, The Chemical Society of Japan (2000) 88.
20. M. Stalzer, *Metalloberfläche* **18** (1964) 263.